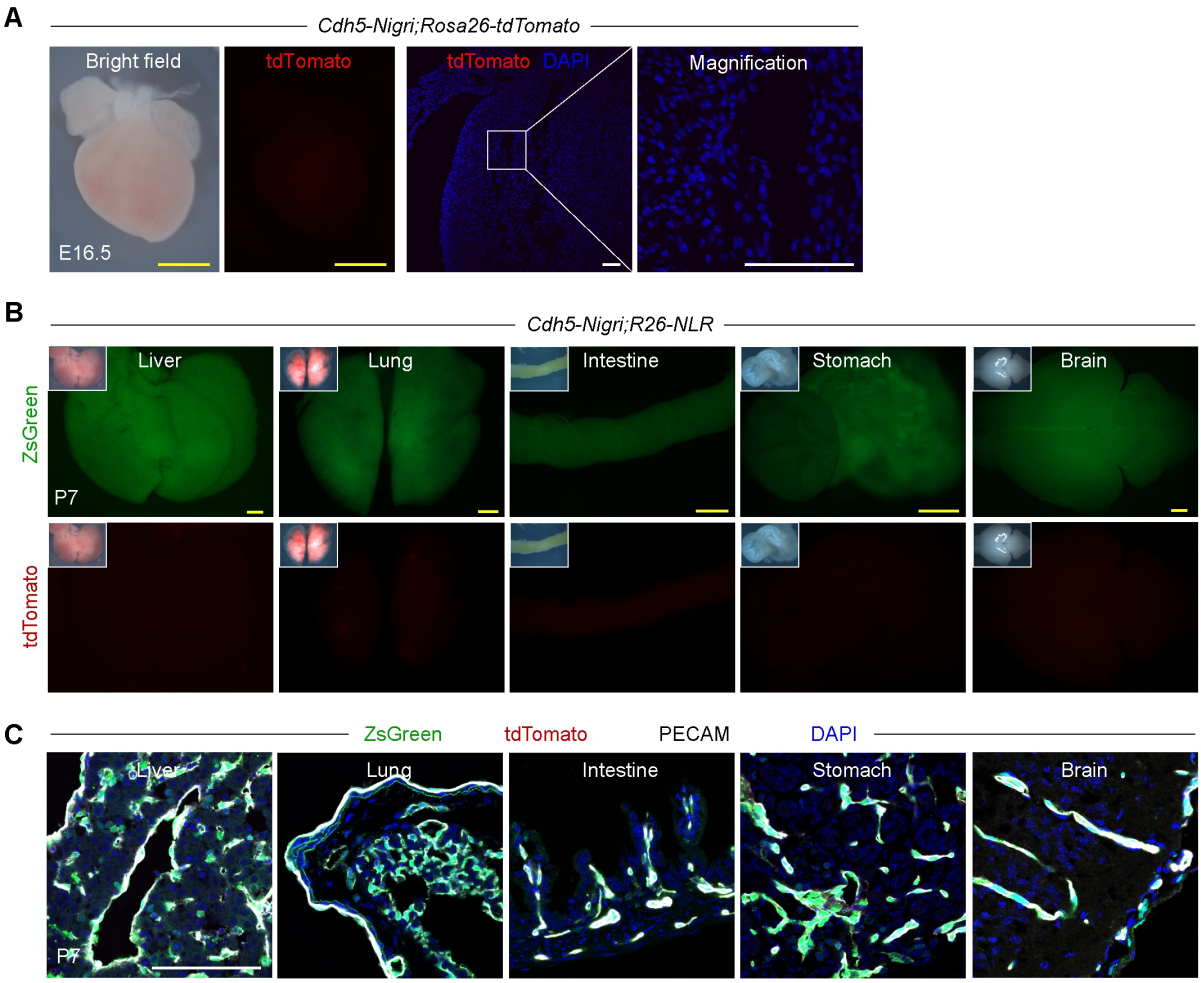

Fig. S1. *Cdh5-Nigri* efficiently and specifically mediated nox sites recombination in endothelial cells *in vivo*. (A) Wholemount views of E16.5 *Cdh5-Nigri;Rosa26-tdTomato* heart. Immunostaining for tdTomato on E16.5 *Cdh5-Nigri;Rosa26-tdTomato* heart shows no cells are tdTomato^{+}. (B) Wholemount views of P7 *Cdh5-Nigri;R26-NLR* organs. (C) Tissues sections from (B) stained for ZsGreen, tdTomato and PECAM shows that PECAM^{+} endothelial cells are ZsGreen^{+}. Yellow bar, 1 mm; white bar, 100 µm. Each image is representative of 4-5 individual biological samples.

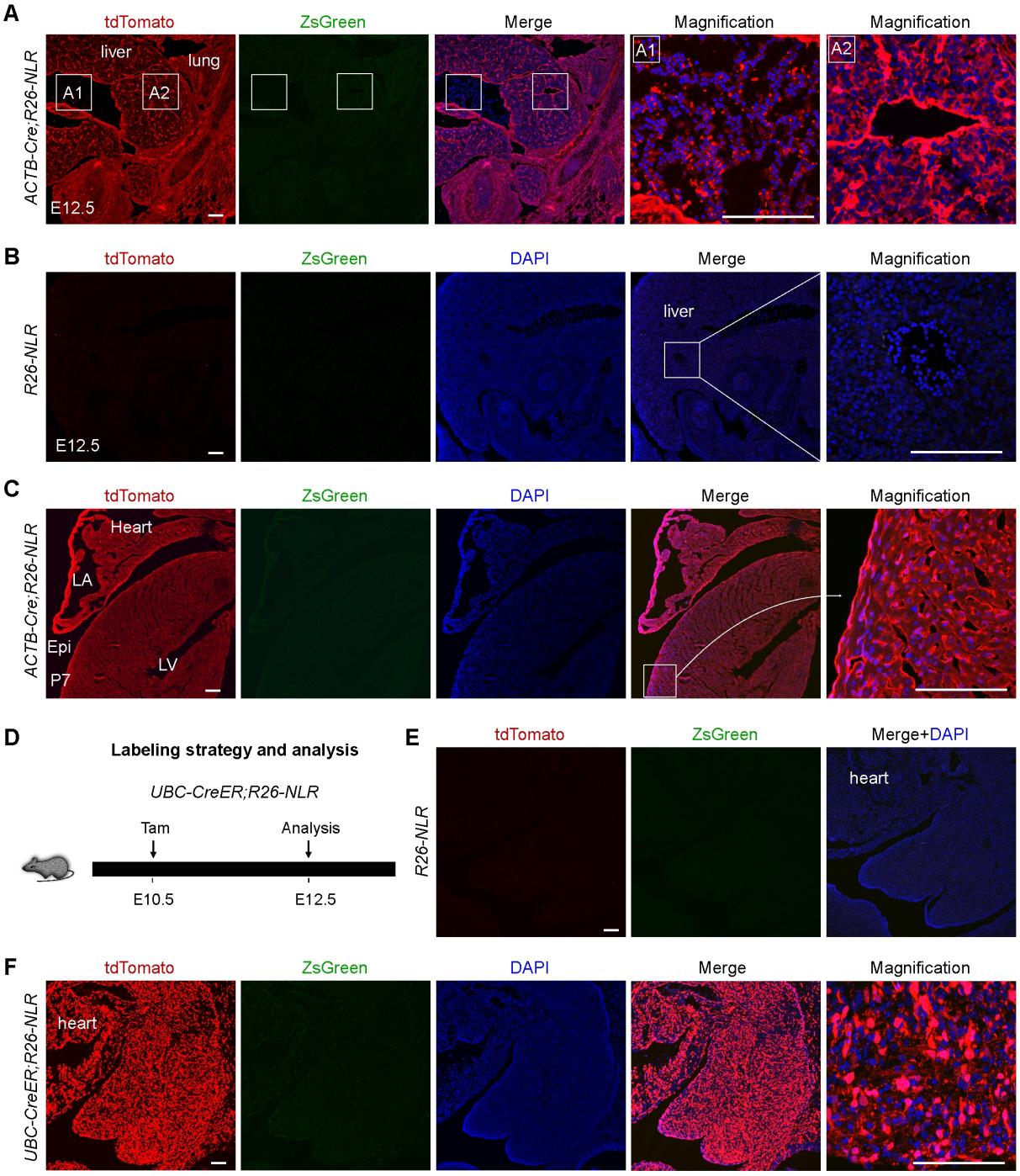

Fig. S2. Cre recombinase efficiently recombines loxP but not nox sites in *R26-NLR* line. (A,B) Immunostaining for ZsGreen and tdTomato on E12.5 *ACTB-Cre;R26-NLR* embryo section shows all cells are tdTomato^{+} (A), and no fluorescent cells in *R26-NLR* embryo (B). (C) Immunostaining for ZsGreen and tdTomato on P7 *ACTB-Cre;R26-NLR* heart section shows all cells are tdTomato^{+}. (D) Schematic image showing experimental strategy. Tamoxifen (Tam) was administered at E10.5 and embryos were collected for analysis at E12.5. (E,F) Immunostaining for ZsGreen and tdTomato on E12.5 *UBC-CreER;R26-NLR* embryo shows all cells are tdTomato^{+} (F), and no fluorescent cells on *R26-NLR* embryo (E). Scale bar, 100 µm. Each image is representative of 4-5 individual biological samples.

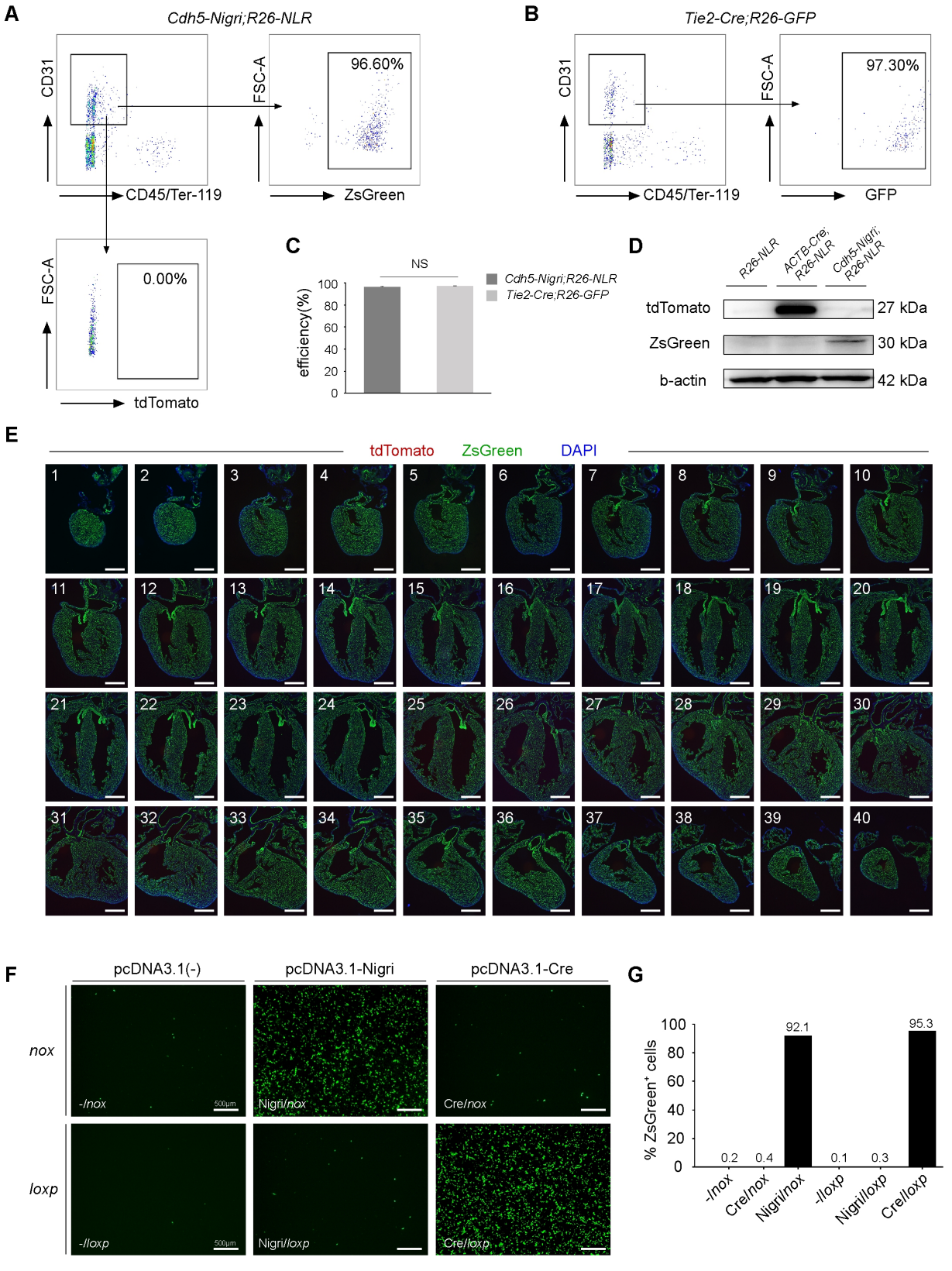

Fig. S3. High efficiency of Nigri-nox and Cre-loxP recombination *in vivo* and negligible crosstalk between Nigri-nox and Cre-loxP systems *in vitro*. (A) Flow cytometric analysis of the percentage of $CD31^+$ endothelial cells labeled by E15.5 *Cdh5-Nigri;R26-NLR* ($ZsGreen^+$) (n=6). (B) Flow cytometric analysis of the percentage of $CD31^+$ endothelial cells labeled by E15.5 *Tie2-Cre;R26-GFP* (GFP^+) (n=6). (C) Quantification results of ZsGreen labeled $CD31^+$ endothelial cells and GFP labeled $CD31^+$ endothelial cells within *Cdh5-Nigri;R26-NLR* and *Tie2-Cre;R26-GFP* tissues. NS, non-significant. (D) Western blot analysis of tdTomato and ZsGreen protein from E15.5 *ACTB-Cre;R26-NLR* and *Cdh5-Nigri;R26-NLR*. *R26-NLR* was used as negative control (n=4). (E) Immunostaining for ZsGreen and tdTomato on serial sections of E15.5 *Cdh5-Nigri;R26-NLR* heart. (F) Recombination analysis between Nigri-nox and Cre-loxP systems after co-transfection of Nigri-expression or Cre-expression plasmids with reporter plasmids. Co-transfections of pcDNA3.1(-) plasmids and reporter plasmids were used as controls. (G) Quantification of recombination efficiency of Nigri-nox and Cre-loxP systems *in vitro* (n=3). Scale bars, 500 μm.

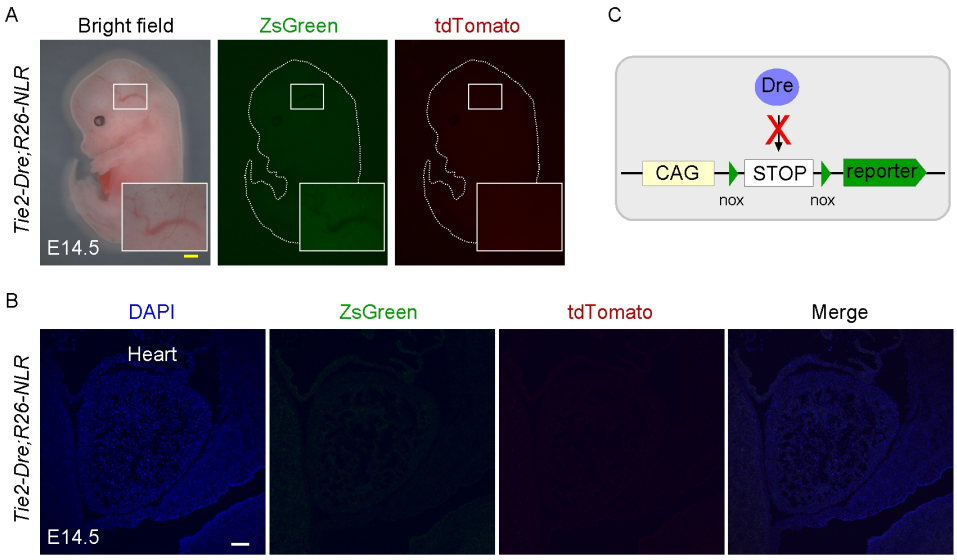

Fig. S4. Dre recombinase can not recombine nox sites in *R26-NLR* line. (A) Wholemount bright-field and epifluorescence views of E14.5 *Tie2-Dre;R26-NLR* embryo. The insets are magnified images of the boxed regions. (B) Immunostaining for ZsGreen and tdTomato on E14.5 *Tie2-Dre;R26-NLR* embryo show no ZsGreen or tdTomato signals detected. (C) Schematic figure showing Dre recombinase can not recognize nox sites in *R26-NLR* line. Yellow bar, 1 mm; white bar, 100 μm. Each image is representative of 4-5 individual biological samples.

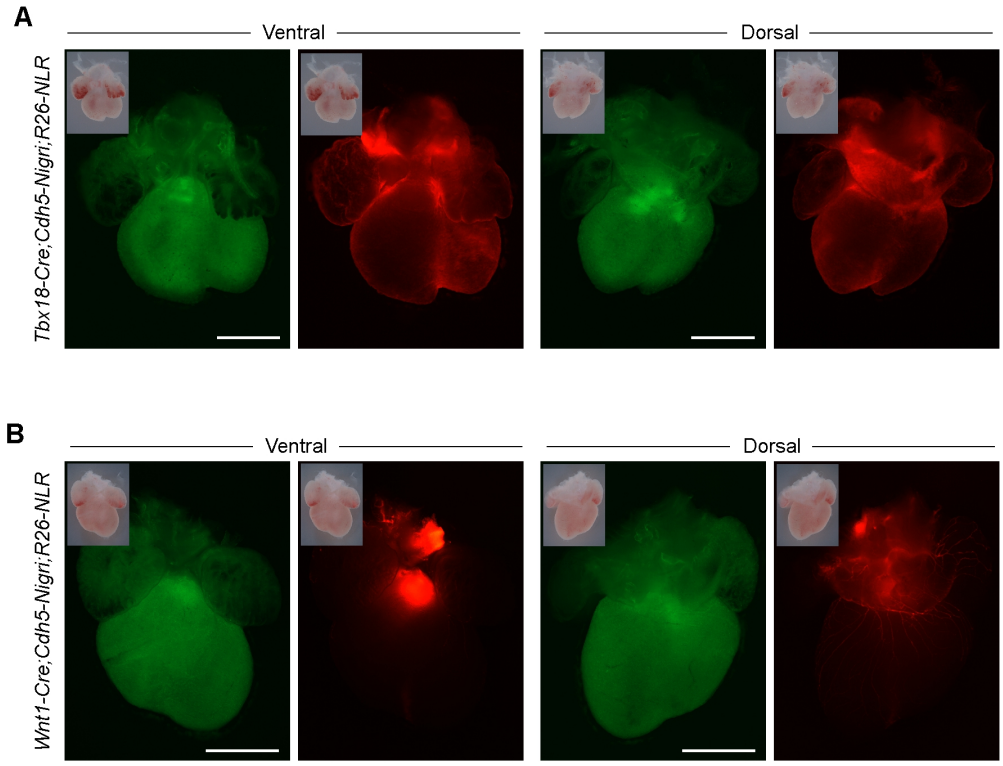

Fig. S5. Simultaneous labeling two genetically distinct progenitor cell populations using *R26-NLR* line. (A) Wholemount views of E14.5 *Tbx18-Cre;Cdh5-Nigri;R26-NLR* embryo showed both expression of tdTomato and ZsGreen in one heart. (B) Wholemount views of E17.5 *Wnt1-Cre;Cdh5-Nigri;R26-NLR* embryo also showed both expression of tdTomato and ZsGreen in one heart. Scale bar, 100 μm. Each image is representative of 4 individual biological samples.